SURFACE VISCOSITY MEASUREMENTS FROM LARGE BILAYER VESICLE TETHER FORMATION

II. Experiments

RICHARD E. WAUGH
Department of Radiation Biology and Biophysics, University of Rochester, School of Medicine and Dentistry, Rochester, New York 14642

ABSTRACT A mechanical experiment has been developed that measures an upper bound for the viscosity of a lipid bilayer membrane. In this experiment, strands of membrane (tethers) are formed from phospholipid vesicles attached to micropipettes by subjecting the vesicles to fluid drag. The rate of tether formation is measured as a function of the velocity of the suspending fluid. The surface viscosity can be calculated from this data using a theoretical relationship derived in a companion paper. Because of the multilamellar character of the vesicles, these values provide an upper bound for the viscosity of a single bilayer. The smallest values obtained in these measurements fell in the range 5.0–13.0 $\times$ 10^{-6} dyn s/cm. These values are in relatively good agreement with the values calculated from lateral and rotational mobility measurements.

INTRODUCTION

The viscosity of a biological membrane is an important factor in determining the rate at which the membrane can undergo deformation on a macroscopic scale, and it also influences the rate at which particles can diffuse in the plane of the surface. These processes play important roles in a wide variety of biological phenomena. Techniques such as flash photolysis and fluorescence photobleaching recovery have been used to study diffusion in membranes. These techniques use molecular probes to measure molecular mobility in the surface. The results invariably reflect the properties of the probe as well as the properties of the membrane system in which they are placed. Moreover, the scope of these measurements is inherently molecular. The relationship between molecular diffusion and macroscopic properties is not clear. The work of Saffman (1976) has provided an important theoretical link between particle mobility and membrane viscosity. However, verification of this theory has not been possible because there has been no macroscopic measurement of bilayer viscosity.

Evans and Skalak (1980) have developed a formulism for the analysis of biological membranes as two-dimensional materials. This framework has been used to analyze the formation of a tether from large point-attached phospholipid vesicles subjected to a fluid drag (Waugh, 1982). The analysis gives the viscosity of the surface in terms of experimentally measurable parameters: the velocity of the suspending fluid, the rate of tether growth, and the diameter of the vesicle. The present report describes the experimental design, the method of calculation and the results.

PROCEDURE

Tethers were formed from large (20.0–65.0 μm diameter) multilamellar vesicles. The vesicles were held with micropipettes and allowed to stick to the pipette tip. The pipette was positioned in the center of a much larger tube (~500 μm i.d.) in a fluid-filled chamber on the microscope stage. The drag force on the vesicle was controlled by adjusting the flow rate in the large tube. The tether was initially formed by increasing the fluid velocity until the body of the vesicle moved away from the pipette tip. Existence of the tether was indicated by a difference between the velocity of the vesicle and the fluid velocity, and by the fact that the vesicle returned to the pipette tip when the fluid velocity fell below some critical value. The fluid velocity at which the vesicle remained stationary is called the equilibrium fluid velocity, v_{fo}. Once v_{fo} was determined, the fluid velocity was suddenly increased, and the velocity of the vesicle, v_v, was recorded along with the fluid velocity v_f. During this part of the measurement a tether was pulled from the body of the vesicle, the rate of tether growth being equal to the velocity of the vesicle. This part of the procedure will be referred to as one "pull." After each pull the equilibrium fluid velocity was measured again to determine whether its value had changed, and then the fluid in the tube was stopped to allow the vesicle to return to the pipette tip. This process was repeated until the tether broke.

Vesicle Preparation

Vesicles were formed from egg phosphatidylcholine (EPC) diluted in hexane to ~2.0 mg/ml. About 5.0 ml of the solution was dried under nitrogen to remove the solvent, after which the lipids were hydrated under water-saturated nitrogen. About 50.0 ml of the suspending medium (either distilled water or 5.0% sucrose solution) was added to the lipid. The suspension was placed in the refrigerator, and vesicles formed spontaneously overnight. Before the experiment, the vesicles were allowed to come to room temperature, 22–25°C.

Microchamber

The chamber in which the vesicles were placed was formed from a U-shaped brass spacer placed between a microscope slide and cover glass

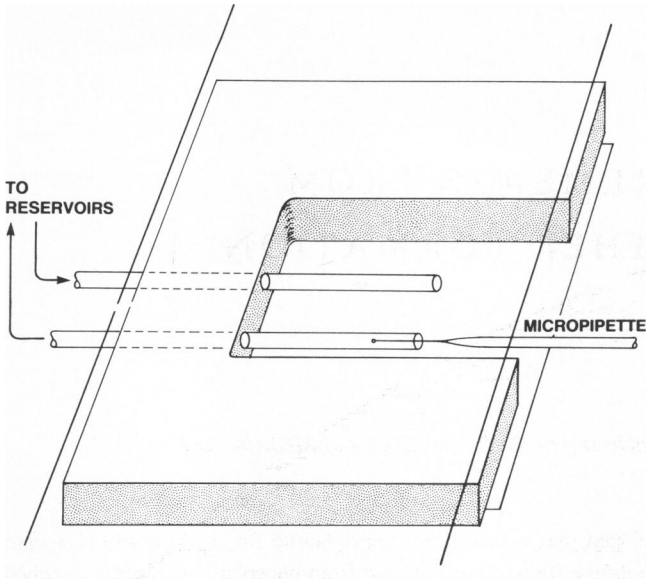

FIGURE 1 Schematic diagram of the chamber in which the experiments were performed. A U-shaped brass spacer formed a cavity between a microscope slide (above) and a cover glass (below). Two lengths of capillary tubing were introduced through the rear of the chamber. A micropipette was inserted through the open side of the chamber into one of the tubes. A vesicle was captured and moved to the center of the tube, and fluid was drawn from the chamber to create a drag force on the vesicle. Fluid flowed into the chamber through the other tube so that the amount of fluid in the chamber remained constant.

and held together with vacuum grease (Fig. 1). This construction formed a cavity (17 mm × 7 mm × 2 mm). A wire from the spacer to the microscope stage insured that no charge difference developed between the vesicles and the pipette. Two capillary tubes were introduced through the rear of the chamber and the micropipette was inserted through the open side (front) of the chamber.

Micropipette

Pipettes were formed from needles pulled from capillary tubing on a vertical pipette puller. The tips were broken off under the microscope to produce an inside diameter between 1.5 and 3.0 μm. Pipettes were filled with suspending fluid by boiling under vacuum. The pipettes were mounted in a DeFonbrune micromanipulator and connected via continuous water connection to a reservoir, the elevation of which could be adjusted with a micrometer drive. The pressure in the pipette (relative to atmosphere) was monitored by a Validyne DP-103 pressure transducer (Validyne Engineering Corp., Northridge, CA) capable of resolving ± 3.0 dyn/cm^2. Zero pressure was determined by aspirating a small particle into the pipette and positioning the reservoir so that the particle was motionless. Because of pressure fluctuations in the chamber due to changes in the curvature of the meniscus, practical resolution of the pressure was $\sim \pm 10.0$ dyn/cm^2.

Control of Fluid Velocity

The two capillary tubes in which the tethers were formed were connected via identical paths to reservoirs mounted on a mechanical device similar to a seesaw, which, when the height of one reservoir was increased, caused the height of the other reservoir to decrease by an equal amount. The difference in the heights of the two reservoirs was controlled by a micrometer drive. The apparatus allowed the upstream and downstream pressures to be changed by equal amounts, so that flow into the chamber through one tube equaled the flow out of the chamber through the other tube. Thus, flow could be induced in the tubes without having fluid flow out the open side of the chamber. The height of the fulcrum of the "seesaw" was adjusted so that the chamber remained full without overflowing. Short lengths of small-diameter tubing ($\sim$50.0 μm i.d.) were placed in the lines from the reservoirs to act as fluid resistors and damp out the effects of small pressure fluctuations in the reservoirs.

Measurement of Fluid Velocity

Direct measurement of the fluid velocity was possible because of many lipid particles contained in the vesicle suspension. However, this approach proved impractical during the experiments because sometimes there were no particles in the field of view and because there were fluid boundary layers around the pipette, the tether, the vesicle and the walls of the tube. To overcome this difficulty, a potentiometer was attached to the micrometer that controlled the flow rate in the tube. The voltage across this potentiometer was proportional to the flow rate. The voltage was calibrated by tracking particles downstream from the pipette in the absence of a tethered vesicle. For very low flow rates the voltage did not provide sufficient resolution because of small fluctuations in the zero voltage. In these cases the velocity was measured directly by tracking particles as far downstream from the vesicle as possible.

The response of the fluid velocity to a step change in reservoir level was obscured by vibrations associated with the turning of the micrometer. When the vibrations stopped, the fluid velocity had already reached its final value. This took $<$0.1 s. All measurements of vesicle velocity were made after the vibrations had stopped.

Microscope

The microscope used in these experiments was a Nikon model M inverted microscope (Nikon, Inc., Instrument Div., Garden City, NY) equipped with Hoffman modulation contrast optics (Modulation Optics, Greenvale, NY). Modulation contrast provides directional contrast enhancement so that the vesicles could be observed within the tube. By aligning the direction of highest contrast with the axis of the tube, the intensities of the leading and trailing edges of the vesicle was maximized while diffraction from the tube walls was minimized.

Television System

A television camera was mounted on the side viewing port of the microscope. The microscope image along with the time, video field number, pressure and flow data were recorded on video tape for subsequent analysis. Distances were measured on the television screen with a vector calculator that produced two cross hairs in the video picture and generated a voltage proportional to the distance between them. Distances were calibrated using the recorded image of a stage micrometer.

CALCULATIONS

The theoretical relationship between the rate of tether growth and the ratio of the fluid velocity to the equilibrium fluid velocity is developed in a companion paper (Waugh, 1982). Two solutions were obtained, one for the case of constant tether diameter, the other for the case where the diameter varied inversely with the axial force. For most of the vesicles studied the scatter in the data was too large to establish which solution more closely predicted the actual behavior. Whenever the resolution was sufficient to distinguish between them, the latter solution matched the results more closely. This is illustrated in Fig. 2. Therefore, the solution based on the assumption that the tether diameter was inversely related to the axial force was used in the calculations.

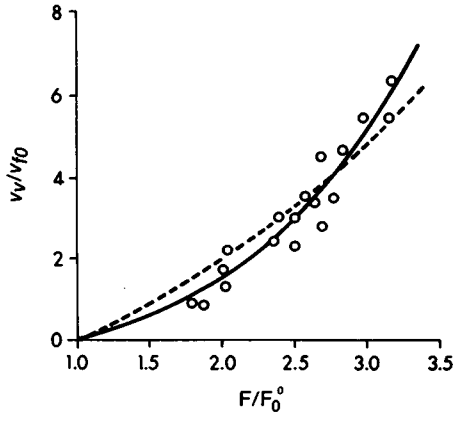

FIGURE 2 The solid line represents the theoretical prediction if the tether diameter varies with axial force; the dashed line is the theoretical prediction if the tether diameter is constant. F/F_o° is the ratio of the force on the vesicle to the force required to maintain constant tether length, v_v is the velocity of the vesicle and v_{fo} is the equilibrium fluid velocity. Circles represent data taken from 17 successive pulls on a single vesicle. The value of the viscosity coefficient determined by single parameter least squares is 109.0×10^{-6} SP for the solid curve and 38.9×10^{-6} SP for the dashed curve. The data correlates better with the solid line prediction.

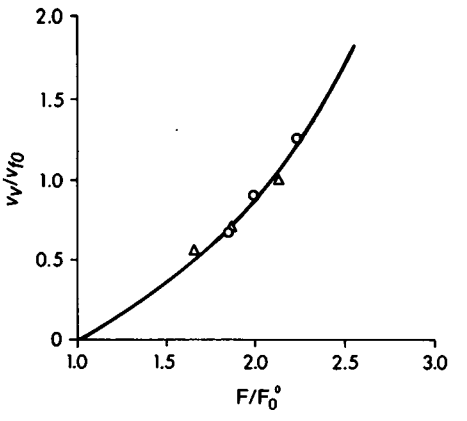

FIGURE 3 Data for two successive pulls on the same vesicle. The velocity of the vesicle decreased from 20.7 to 16.3 μm/s during one pull (triangles) and from 26.0 to 19.2 μm/s during the second pull (circles). Values used for the equilibrium fluid velocity were calculated from Eq. 3 and ranged from 20.9–29.5 μm/s for the first pull, and 20.6–28.5 μm/s for the second pull. All data points are consistent with a value of 99.0×10^{-6} SP for the surface viscosity.

In the analysis an assumption was made that the pressure difference across the bilayer remains constant. This assumption can be tested experimentally. The pressure difference, ΔP, is related to the force required to maintain constant tether length, F_o° (Waugh, 1982):

$$\Delta P = \frac{F_o^\circ}{\pi r_t^\circ R_v}, \tag{1}$$

where r_t° is the radius of the tether and R_v is the radius of the vesicle. The critical force, F_o°, is in turn related to the equilibrium fluid velocity, v_{fo}, via Stokes's equation:

$$F_o^\circ = 6\pi R_v \mu v_{fo}, \tag{2}$$

where μ is the viscosity of the suspending medium. Thus, changes in the equilibrium fluid velocity, v_{fo}, reflect changes in the pressure difference across the membrane, ΔP.

In practice the pressure (as reflected by the equilibrium fluid velocity, v_{fo}) was found to increase with tether length. As the change in v_{fo} was usually small compared with the rate of tether growth, quasi-steady state could be assumed, and an appropriate intermediate value for the equilibrium fluid velocity was used in the calculation. The value of v_{fo} was determined by interpolation according to the following expression:

$$v_{fo} = v_{fo}(\text{start}) + \frac{L(v_v) - L(\text{start})}{L(\text{end}) - L(\text{start})} \cdot \left[v_{fo}(\text{end}) - v_{fo}(\text{start})\right], \tag{3}$$

where v_{fo}(start) and L(start) represent the equilibrium fluid velocity and tether length before the pull, v_{fo}(end) and L(end) represent the quantities after the pull, and $L(v_v)$ represents the length of the tether at which the vesicle velocity is measured. The success of this approach is illustrated in Fig. 3, which shows three successive measurements on each of two pulls for the same vesicle. Different values for v_v and v_{fo} were used for each point, yet the value of the viscosity is consistent within each pull and from one pull to the next.

In cases where more than one pull was performed on a given vesicle, two approaches were used to determine a single value for the surface viscosity. The simplest method was to calculate a value for each individual pull and average the results. This method had the advantage that a standard deviation could be calculated to provide a quantitive measure of the scatter for each vesicle. The other approach was to use a single parameter least-squares routine. The value for the viscosity, η, was chosen that minimized the following quantity:

$$\sum\left[\frac{8\pi\eta v_v}{F_o^\circ} - G^\circ(Q)\right]^2.$$

The equilibrium force, F_o°, is calculated from the measured value of the equilibrium fluid velocity, v_{fo}, via Stokes's drag equation (Eq. 2). Thus the first term in the expression represents the measured value of the dimensionless tether growth parameter, G°. The second term represents the theoretical value for G° based on the measured force ratio,

$$Q = F/F_o^\circ = \frac{v_f - v_v}{v_{fo}}. \tag{4}$$

This approach gives more weight to pulls where the

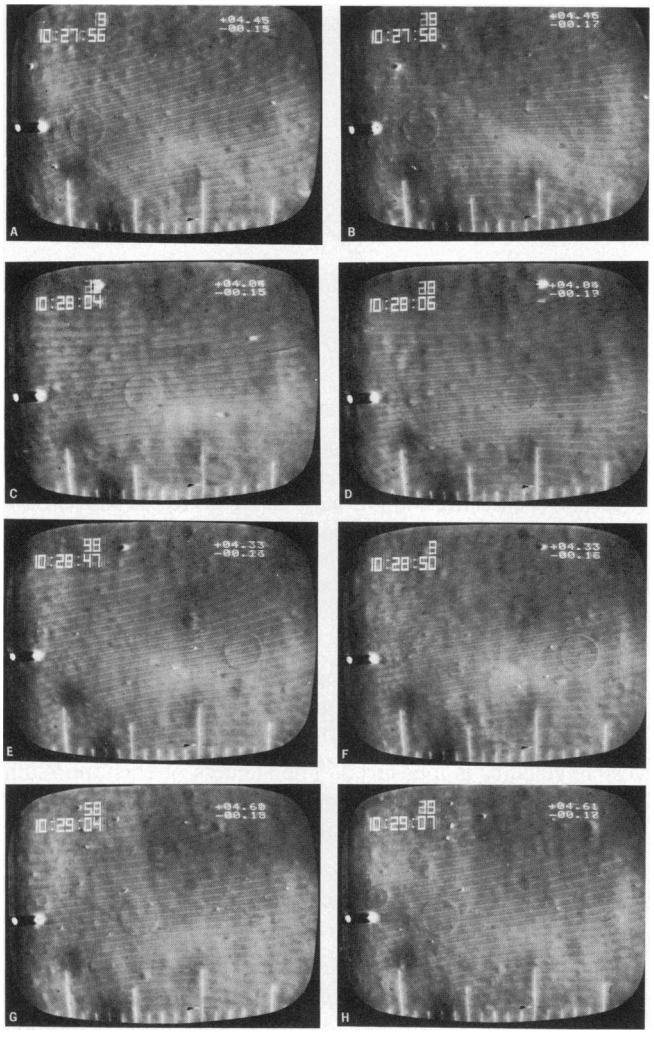

FIGURE 4 Photographs of vesicle tether formation. Numbers in the upper left give the time and video frame number; numbers at the upper right are related to fluid velocity and pipette pressure. The pipette tip is visible at the left of the screen. Each scale division is ~10.0 μm. *A* and *B*: the vesicle is stationary; the fluid velocity is v_{fo}(start). *C* and *D*: the vesicle is moving at a velocity, v_v, and the fluid velocity is v_f. *E* and *F*: the vesicle is stationary; the fluid velocity is v_{fo}(end). *G* and *H*: the fluid velocity is $<v_{fo}$; the vesicle is returning to the pipette tip.

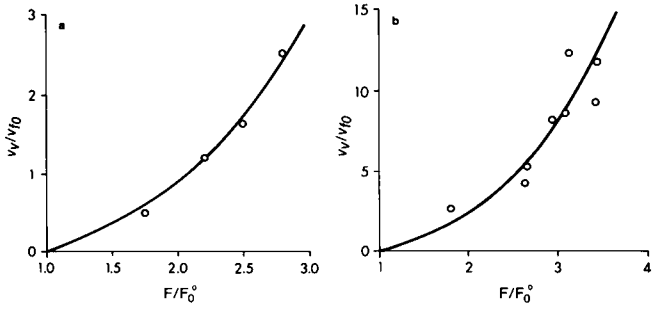

FIGURE 5 A few vesicles exhibited discontinuities in the measured value of the viscosity during successive pulls. (*a*) Data for the first four pulls on this vesicle are consistent with a viscosity of 140.0 × 10^{-6} SP. (*b*) Data for the last eight pulls on the same vesicle are consistent with a viscosity of 51.5 × 10^{-6} SP.

measured velocities are large and the fractional error in their measurement should be smaller. Generally, for a given vesicle the values determined by these methods did not differ significantly. The values presented in the remainder of the paper are those determined by the least-squares method, unless otherwise specified.

RESULTS

Photographs of the tether pulling sequence are shown in Fig. 4. The first pair shows the vesicle tethered to the pipette before the pull. The motion of the fluid is indicated by the change in the position of particles suspended in the fluid. The fact that the vesicle is stationary indicates the existence of the tether, which cannot be seen. The velocity of the fluid is v_{fo}(start) which is used in Eq. 3. The second pair of photographs shows the tether pull. Note that although the vesicle is moving, the vesicle velocity (v_v) is not as great as the fluid velocity (v_f). In the third pair of pictures the vesicle is again stationary; the value of the fluid velocity is v_{fo}(end). Finally, the last pair of photographs shows that when the fluid velocity is less than v_{fo} the vesicle returns to the tip of the pipette, as was predicted by the analysis.

Measurements were performed on a total of 42 vesicles. Of these, there were three that exhibited extremely wide fluctuations in the calculated value of the viscosity, and three others for which the calculated value progressively and markedly decreased. Measurements on these six vesicles were discarded, because the proper value for the surface viscosity could not be identified with any confidence. Of the remaining 36, 4 showed clear discontinuities in their behavior and have been counted as two independent determinations. The number of pulls for each determination ranged from 1 to 21, and in some cases multiple points were taken for the same pull. The 40 viscosity determinations represent a total of 209 pulls and 251 data points. Values for the viscosity ranged from 5.0 × 10^{-6} to 1.7 × 10^{-4} dyn s/cm (surface poise, SP).

A wide range of viscosity values is expected because of the multilamellar character of the vesicles. This character is indicated by the discontinuous behavior of some of the vesicles. Fig. 5*a* and *b* shows best fits for a single vesicle. Fig. 5*a* shows that the first four pulls are consistent with a viscosity coefficent of 140.0 × 10^{-6} SP, whereas Fig. 5*b* shows that the last eight pulls are consistent with a viscosity of 51.5 × 10^{-6} SP. During the time between these determinations, a distinct break in the motion of the vesicle was observed. The obvious explanation for these observations is that a portion of the surface (some but not all of the layers) gave way, and in subsequent pulls did not contribute to the surface dissipation. This kind of phenomenon was observed several times in the course of the experiments. In two cases the membrane continued to disintegrate (i.e., the measured viscosity progressively decreased) during subsequent pulls. When the membrane

failed to restabilize, the subsequent pulls were discarded. At no time was the viscosity observed to increase discontinuously during a series of measurements.

In a multilamellar system the measured value of the viscosity should vary according to the number of layers included in the tether. If the layers behave independently, the measured viscosity coefficient would be the sum of the coefficients for all contributing layers. In the case when each layer had the same viscosity, the measured value, η_m would be the product of the viscosity of a single layer, η_{BL}, and the number of layers in the tether, n: $\eta_m = n\,\eta_{BL}$. Thus, for independent layers a periodic distribution in the measured values of the viscosity would be expected. If the layers are not independent, clustering of the measured values would still be expected, but the clusters might not occur at uniform intervals.

A histogram of the measured values is shown in Fig. 6. Although the data are spread over a wide range, some clustering can be seen. Six values lie in the interval 12.0–18.0 $\times$ 10^{-6} SP, seven fall in the range 24.0–33.0 $\times$ 10^{-6} SP, and six fall in the range 42.0–53.0 $\times$ 10^{-6} SP. The data are insufficient in quantity and resolution to specify the cluster intervals with confidence. It is possible, for example, that the group at 24.0–33.0 $\times$ 10^{-6} SP might actually be two groups, one centered around 24.0 $\times$ 10^{-6} SP and one centered around 33.0 $\times$ 10^{-6} SP. The fact that the values fall in clusters supports the contention that the wide range of measured values may be due to differences in the number of layers incorporated into the tethers.

If the large measured values of the viscosity were due to a large number of layers in the tether, the tether radius would have been quite large (on the order of 0.5 μm). Such a large tether might be visible under the microscope. Unfortunately, it would not have been possible to see the tethers during the experiment because of the directional quality of modulation contrast. To see the tethers, the direction of maximum contrast must be aligned perpendicular to the axis of the tether. Because the tether axis is parallel to the axis of the tube in which the experiments were performed, refraction from the tube walls would have obliterated the image of the tether. Attempts to see tethers formed outside of the tube were not successful.

It should be pointed out that the value of the viscosity calculated from the data depends strongly on which solution to the tether growth problem is used (Waugh, 1982), i.e., whether the tether radius is assumed to vary with the force on the vesicle or to be constant. The tether has been assumed to vary with the force for two reasons: first, the radii of tethers pulled from erythrocytes have been found to depend on axial force (Hochmuth et al., 1981); and second, whenever there was sufficient resolution in the data (~10% of the time), the solution based on a variable tether radius seemed to match the results more closely (Fig. 2). Although these observations are strong indications that the tether radius does vary with axial force, they do not constitute proof. Therefore, values for the viscosity based on the assumption that the tether radius is constant are shown in Fig. 7. The values range from 2.7 $\times$ 10^{-6} to 88.0 $\times$ 10^{-6} SP. There are clusters of values near 6.0 $\times$ 10^{-6} and 12.0 $\times$ 10^{-6} SP. These calculated values are somewhat smaller than those calculated under the assumption that the tether radius varies with the axial force.

Measurement Error

Most of the scatter within a given cluster, and between successive pulls on the same vesicle can be attributed to

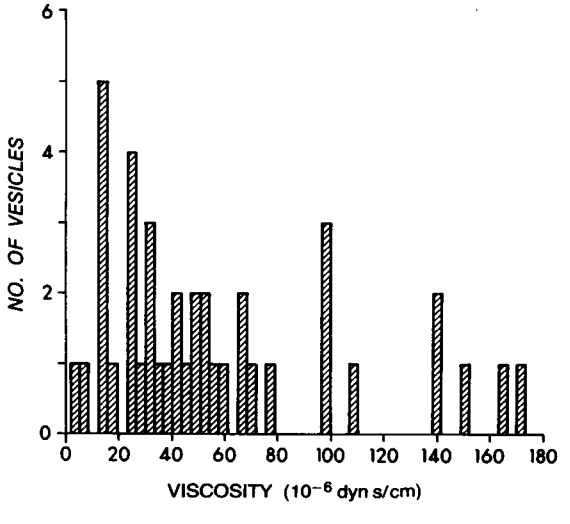

FIGURE 6 Histogram showing the distribution of viscosity values for the experiment. The values were calculated under the assumption that the tether radius was inversely proportional to the axial force. A total of 40 determinations were made. The wide range of measured values reflects the multilamellar character of the vesicles. Note the clustering of values ~12.0–15.0, 25.0–30.0 and 50.0 $\times$ 10^{-6} SP.

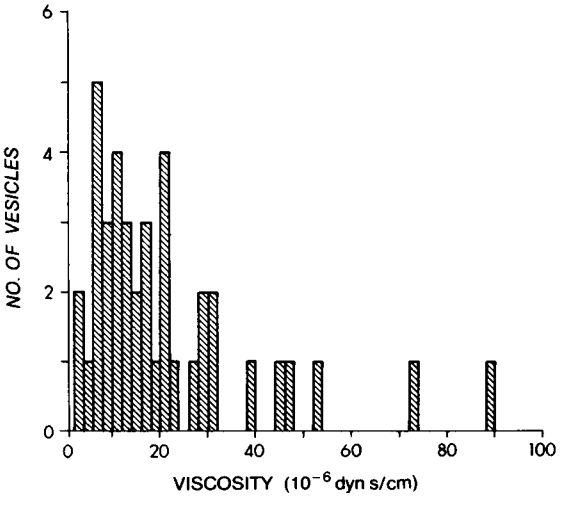

FIGURE 7 Distribution of measured values of the viscosity calculated under the assumption that the tether radius was constant. The data are the same as those represented in Fig. 6; only the method of calculation is different.

measurement error. Three quantities are important for determining the value of the viscosity: the equilibrium fluid velocity, v_{fo}, the velocity of the vesicle during the pull, v_v, and the fluid velocity during the pull, v_f. It is possible to estimate the fractional error in the measured value of the viscosity for a fractional error in each of these quantities. For values of $Q > 1.5$, the tether growth parameter, G_R^o, is approximately equal to Q^3 (Waugh, 1982):

$$G^o = \frac{8\pi\eta_m v_v}{F_o^o} \simeq \left[\frac{(v_f - v_v)}{v_{fo}}\right]^3, \qquad Q \geq 1.5. \quad (5)$$

Solving for η_m we find:

$$\eta_m = C \cdot \frac{(v_f - v_v)^3}{v_v v_{fo}^2}, \quad (6)$$

where C is a constant. The change in η_m due to small changes in each of the measured parameters is obtained from the differential expansion of η_m in terms of these quantities:

$$d\eta_m = C\left\{\frac{3(v_f - v_v)^2}{v_v v_{fo}^2} dv_f - \left[\frac{3(v_f - v_v)^2}{v_v v_{fo}^2} + \frac{(v_f - v_v)^3}{v_v^2 v_{fo}^2}\right] dv_v - \frac{2(v_f - v_v)^3}{v_v v_{fo}^3} dv_{fo}\right\}. \quad (7)$$

To obtain the fractional change in η_m in terms of the fractional error in the measured velocities, we divide Eq. 7 by Eq. 6:

$$\frac{d\eta_m}{\eta_m} = \left[\frac{3}{1-\xi}\right]\frac{dv_f}{v_f} - \left[\frac{2\xi + 1}{1-\xi}\right]\frac{dv_v}{v_v} - 2\frac{dv_{fo}}{v_{fo}}, \quad (8)$$

where ξ is the ratio of the vesicle velocity to the fluid velocity, v_v/v_f. Note that $0.0 \leq \xi < 1.0$.

The accuracy of the velocity measurements depends on the accuracy with which the position of a particle in the fluid could be determined as a function of time. Resolution of the time measurement was limited by the field rate of the video system or 1/60 s. The time interval was typically 1.0 s, so the expected error in the time was ± 2.0%. Practical resolution of position was between ± 0.5 and ± 1.0 μm. The distance that particles travelled was typically 50.0 μm or more, making the expected error ± 2.0% or less. The maximum expected error in the velocity is the sum of these errors, or ~±4.0%. This is a reasonable estimate of the possible error in the vesicle and fluid velocities.

Estimation of the expected error in the equilibrium fluid velocity measurement is complicated by the fact that it often increased with increasing tether length. The size of the increase varied considerably from vesicle to vesicle. In some cases v_{fo} was essentially constant, but in rare cases it could as much as triple during the course of a single pull. A doubling in the value of v_{fo} was not uncommon during long pulls. Generally, if a strong dependence of v_{fo} on tether length was observed, it persisted throughout all measurements performed on the vesicle. It is difficult to quantify the potential error introduced by the approximation given in Eq. 3. It seems reasonably certain, however, that in most cases the value used in the calculations is not in error by >15%.

Based on these estimates of the uncertainty in the measured parameters it is possible to estimate the expected fluctuation in the calculated viscosity from measurement error via Eq. 8. For values of the viscosity $<35.0 \times 10^{-6}$ SP, the value of the velocity ratio, ξ, fell betwen 0.4 and 0.8. Therefore, a 4.0% error in the fluid velocity, v_f, would have resulted in an error in the calculated viscosity of between 20.0 and 60.0%; a 4.0% error in the vesicle velocity, v_v, would have resulted in an error in the viscosity of between 12.0 and 52.0%; and a 15.0% error in the equilibrium fluid velocity, v_{fo} would have resulted in an error of 30.0%. These estimates of the effects of measurement error demonstrate that meaningful results can be obtained only when extreme care is taken in the data analysis. They also show that measurement error cannot account for the wide range of viscosities measured in these experiments, although it can account for most of the scatter among measurements made on an individual vesicle.

Another potential source of error in a multilamellar system is the possibility of frictional interaction between the outer surface, which flows into the tether, and supporting layers beneath it. It is difficult to estimate the magnitude of the error that this might introduce, but it would certainly increase the apparent value of the surface viscosity. Such frictional interactions could account for some of the very large measured values. Since these interactions would only increase the measured value, these measurements can still be regarded as an upper bound to the viscosity of a single bilayer.

DISCUSSION

In the analysis of tether formation (Waugh, 1982) it was pointed out that quite different behavior would be expected in the formation of tethers from spherical and nonspherical vesicles. Tether formation from a spherical vesicle requires a change in the volume of the vesicle, since incorporation of material into the tether reduces the surface area of the spherical region. A calculation was performed which showed that the permeability of the vesicle surface is not large enough for this volume change to occur during the time it takes to pull the tether. It was concluded that tethers could not be formed from perfectly spherical vesicles except at extremely slow rates, and therefore, the vesicles in these experiments must not be perfectly spherical. Since the volume of the vesicle cannot change during tether formation, the osmotic properties of

the vesicle interior and the suspending solution should have no effect on tether formation. During the experiments no differences were observed between vesicles formed in 5.0% sucrose and those formed in distilled water. This observation supports the conclusion that there was sufficient excess surface area in the vesicles to form tethers without decreasing the vesicle volume.

The conclusion that the vesicles are not spherical raises questions about the origin of the transmembrane pressure difference. The magnitude of the pressure difference can be estimated from the equilibrium fluid velocity, v_{fo}, from Eqs. 1 and 2. Based on an estimate of tether radius of 1.0×10^{-6} cm, the pressure difference in these experiments was calculated to be between 25 and 250 dyn/cm^2. Although this is a very small pressure, it is much too large to be supported by a single bilayer in a nonspherical geometry because the bilayer has no shear rigidity and its bending rigidity is very small (Evans and Skalak, 1980). The pressure cannot arise from hydrodynamic forces, since these forces are small compared to the pressure force (Waugh, 1982, Appendix). We conclude, therefore, that the nonspherical geometry is probably supported by multilamellar structures beneath the outer surface. Increases in the value of v_{fo} with increasing tether length probably reflect small deformations of these underlying layers as material is drawn from the vesicle into the tether at constant vesicle volume. If the tether were to become long enough, the excess area of the vesicle would be used up, and tether growth would presumably stop. However, because it takes so little material to form a tether, it is unlikely that this point would be reached within the view field of the microscope. Such a stopping point was never observed during the experiments.

Because of the multilamellar character of the vesicles, these measurements provide an upper bound for the viscosity of a single bilayer. Based on the data, this upper bound lies in the range, 5.0–13.0 $\times 10^{-6}$ SP (dyn s/cm). It is interesting to compare this value to the values calculated from molecular mobility measurements. The theoretical relationship between lateral (D_L) and rotational (D_R) mobility and surface viscosity has been obtained by Saffman (1976):

$$D_L = \frac{kT}{4\pi\eta}\left[\ln\left(\frac{\eta}{\mu a}\right) - 0.577\right] \tag{9a}$$

$$D_R = \frac{kT}{4\pi a^2\eta}. \tag{9b}$$

Here, the surface viscosity, η, replaces the product of the membrane bulk viscosity times the membrane thickness in Saffman's original equations. (See Evans and Hochmuth, 1978.) The viscosity of the suspending medium, μ, is assumed to be much less than the membrane viscosity; k is Boltzman's constant and T is absolute temperature. These relationships (Eq. 9) are based on the model of a cylindrical particle of radius, a, which spans the thickness of the membrane.

Some measurements of lateral diffusion coefficients are summarized in Table I, along with corresponding values for the surface viscosity calculated via Saffman's equations. There are some important considerations to be made when using Saffman's equations to obtain values for the surface viscosity. First, it should be emphasized that Eq. 9 a and b are only valid for particles that span the thickness of the membrane. It is not clear how they should be applied to particles that penetrate only a fraction of the bilayer. This is illustrated by the measurements on glycophorin and gramicidin-S in the same type of membrane and by the same investigator. The viscosity calculated for the membrane spanning protein (glycophorin) is significantly higher than the viscosity calculated for gramicidin-S, which spans only half of the bilayer. A second consideration is the importance of comparing similar membrane systems. This is illustrated by the measurements using the probe *N*-4-nitrobenz-2-oxa-1,3-diazole phosphatidylethanolamine (NBD-PE). The value of the diffusion coef-

TABLE I
LATERAL MOBILITIES

Diffusing species	Membrane type (temperature)	D_L	a	η^*	Reference
		10^{-9}cm^2/s	nm	10^{-6}SP	
Rhodopsin	Disk (20°C)	4.0	2.0	6.1	Poo and Cone (1974) Liebman and Entine (1974)
Band 3	RBC‡ (37°C, low salt)	2.0	2.0	13.4	Golan and Veatch (1980)
DiI	RBC (37°C)	6.0	0.5	4.7	Kapitza and Sackman (1980)
Glycophorin	EPC (24°C)	20.0	0.5	1.2	Wu et al. (1981)
NBD PE	Reconstituted *E-coli* Phospholipid (24°C)	1.5	0.47	22.0	Schindler et al. (1980)
NBD PE	DMPC (26°C)	50.0	0.47	0.4	Smith et al. (1979)
Gramicidin S	EPC (24°C)	35.0	0.47	0.6	Wu et al. (1978)
NBD PE	EPC (25°C)	40.0	0.47	0.53	Wu et al. (1977)

*Calculated, Eq. 9a.
‡RBC, red blood cell.

ficient ranges from 1.5×10^{-9} to 5.0×10^{-8} cm^2/s in the three membrane systems studied. Finally, it is important to consider the dependence of the mobility on particle size. The rotational mobility is very sensitive to particle size, as it varies inversely with the square of the particle radius. On the other hand, the lateral mobility is relatively insensitive to particle size, as it depends only on the logarithm of the radius. An accurate measurement of the radius of that part of a probe that spans the membrane is absolutely necessary to obtain reliable estimates of surface viscosity from rotational diffusion measurements. On the other hand, lateral mobility measurements can provide reliable estimates of the surface viscosity even when accurate measurements of molecular dimensions are not available.

It is interesting that the viscosity calculated from the diffusion of glycophorin, which spans the membrane, is almost exactly twice that calculated from the measurements on gramicidin-S, which spans half of the membrane. This observation makes sense if the two halves of the bilayer are hydrodynamically uncoupled, that is, if diffusion of a particle in one half of the bilayer does not require movement of molecules in the other half of the bilayer. The diffusion of a probe spanning one half of the bilayer would be limited by dissipation in only that half of the bilayer, whereas the diffusion of a membrane spanning protein would produce dissipation in both halves of the bilayer. Thus, the apparent membrane viscosity calculated from the diffusion of a probe that spans half of the membrane ought to be half of the apparent membrane viscosity calculated from the diffusion of a membrane spaning probe. This rule of thumb should be applicable to membranes that are symmetric and have no peripheral structures such as glycocalyx or cytoskeleton. Naturally, the rate of diffusion of a probe in a membrane with such structures depends on the amount of interaction between the probe and the structure.

Although calculation of surface viscosity from rotational diffusion coefficients is prone to errors due to the strong dependence of the result on particle size, there is one measurement of rotational diffusion on a well-characterized membrane-spanning molecule. The molecular diameter of bacteriorhodopsin has been determined by Henderson and Unwin (1975) to be 3.0 ± 0.7 nm. Cherry (1977) has measured the rotational diffusion of bacteriorhodopsin in dimyristoylphosphatidylcholine (DMPC) bilayers by flash photolysis. Using Cherry's value for the rotational diffusion coefficient ($D_R = 1.0 \times 10^{-5}$ s^{-1}), and a molecular radius of 1.5 nm, the surface viscosity is calculated (Eq. 9b) to be 1.5×10^{-6} SP. This is in good agreement with the value calculated from the lateral diffusion measurements of Wu et al. (1981).

The surface viscosity obtained from mechanical measurements reflects the composite properties of the surface being drawn into the tether. If the surface comprises a single EPC bilayer, and if Saffman's relationships are correct, the mechanically determined value should equal the value calculated from the diffusion coefficient of membrane-spanning proteins in phospholipid bilayers, $1.2–1.5 \times 10^{-6}$ SP. The fact that the mechanically measured values are greater than the value calculated from diffusion measurements is not surprising as the mechanical measurements constitute an upper bound to the viscosity of a single bilayer. The difference between the mechanically measured value and the one calculated from diffusion measurements should not be regarded as disproof of Saffman's theory. The multilamellar character of the vesicles, the effect of measurement errors at low viscosity, and uncertainty about the dependence of tether radius on axial force make it difficult to draw definite conclusions. Regardless of the validity of Saffman's theory, these mechanical measurements establish an upper bound for the viscosity of a single phospholipid bilayer of 5.0×10^{-6} SP.

The author would like to thank Dr. Thomas Murphy for his instructions in preparing large vesicles, and Dr. Francis Kirkpatrick who supplied the phosphatidylcholine and the rotoevaporator used in the experiments.

This work was supported in part by National Institutes of Health grants HL-07152 and HL-16421. This paper is based on work performed under contract DE-AC02 76EV03490 with the U.S. Department of Energy at the University of Rochester Department of Radiation Biology and Biophysics and has been assigned Report No. UR-3490-1958.

Received for publication 26 January 1981 and in revised form 2 June 1981.

REFERENCES

Cherry, R. F., U. Muller, and G. Schneider. 1977. Rotational diffusion of bacteriorhodopsin in lipid membranes. *FEBS (Fed. Eur. Biochem. Soc.) Lett.* 80:465–469.

Evans, E. A., and R. M. Hochmuth. 1978. Mechanochemical properties of membranes. *Curr. Top. Membr. Transp.* 10:1–62.

Evans, E. A., and R. Skalak. 1980. Mechanics and Thermodynamics of Biomembranes. CRC Press, Inc., Boca Raton, FL.

Golan, D. E., and W. Veatch. 1980. Lateral mobility of band 3 in the human erythrocyte membrane studied by flourescence photobleaching recovery: evidence for control by cytoskeletal interactions. *Proc. Natl. Acad. Sci. U.S.A.* 77:2537–2541.

Henderson, R., and P. N. T. Unwin. 1975. Three-dimensional model of purple membrane obtained by electron microscopy. *Nature (Lond.).* 257:28–32.

Hochmuth, R. M., H. C. Wiles, and E. A. Evans. 1981. Mechanical measurement of membrane thickness. *Biophys. J. (Abstr.)* 33:177*a*.

Kapitza, H. G., and E. Sackmann. 1980. Local measurement of lateral motion in erythrocyte membranes by photobleaching technique. *BBA (Biochem. Biophys. Acta) Libr.* 595:56–64.

Liebman, P. A., and G. Entine. 1974. Lateral diffusion of visual pigment in photoreceptor disk membranes. *Science (Wash., D.C.).* 185:457–459.

Poo, M., and R. A. Cone. 1974. Lateral diffusion of rhodopsin in the photoreceptor membrane. *Nature (Lond.).* 247:438–441.

Saffman, P. G. 1976. Brownian motion in thin sheets of viscous fluid. *J. Fluid Mech.* 73:593–602.

Schindler, M., M. J. Osborn, and D. E. Koppel. 1980. Lateral mobility in reconstituted membranes: comparisons with diffusion in polymers. *Nature (Lond.)*. 283:346–350.

Smith, L. M., J. W. Parce, B. A. Smith, and H. M. McConnell. 1979. Antibodies bound to lipid haptens in model membranes diffuse as rapidly as the lipids themselves. *Proc. Natl. Acad. Sci. U.S.A.* 76:4177–4179.

Waugh, R. E. 1982. Surface viscosity measurements from large bilayer vesicle tether formation. I. Analysis. *Biophys. J.* 38:19–27.

Wu, E., K. Jacobson, and D. Papahadjopoulos. 1977. Lateral diffusion in phospholipid multibilayers measured by flourescence recovery after photobleaching. *Biochemistry*. 16:3936–3941.

Wu, E., K. Jacobson, F. Szoka, and A. Portis, Jr. 1978. Lateral diffusion of a hydrophobic peptide, *N*-4-nitrobenz-2-oxa-1,3-diazole gramicidin S, in phospholipid multibilayers. *Biochemistry*. 17:5543–5549.

Wu, E. S., P. S. Low, and W. W. Webb. 1981. Lateral diffusion of glycophorin reconstituted into phospholipid multibilayers. *Biophys. J.* (*Abstr.*) 33:109*a*.